3D MOUTH TRACKING FROM A COMPACT MICROPHONE ARRAY CO-LOCATED WITH A CAMERA

Xinyuan Qian[1], *Alessio Xompero*[1], *Alessio Brutti*[2], *Oswald Lanz*[2], *Maurizio Omologo*[2], *Andrea Cavallaro*[1]

[1]Centre for Intelligent Sensing, Queen Mary University of London, UK
[2]ICT-irst, Fondazione Bruno Kessler, Trento, Italy

ABSTRACT

We address the 3D audio-visual mouth tracking problem when using a compact platform with co-located audio-visual sensors, without a depth camera. In particular, we propose a multi-modal particle filter that combines a face detector and 3D hypothesis mapping to the image plane. The audio likelihood computation is assisted by video, which relies on a GCC-PHAT based acoustic map. By combining audio and video inputs, the proposed approach can cope with a reverberant and noisy environment, and can deal with situations when the person is occluded, outside the Field of View (FoV), or not facing the sensors. Experimental results show that the proposed tracker is accurate both in 3D and on the image plane.

Index Terms— Audio-visual fusion; particle filter; 3D tracking.

1. INTRODUCTION

Tracking the position of a person is a fundamental task for scene understanding, human-machine and human-robot interaction. Tracking can be carried out on the image plane [1–4], on a ground plane [5] or in 3D [6–9]. Methods for tracking a person in 3D generally use spatially distributed camera networks and microphone arrays. However, the use of robotic assistants and smart-home devices, such as Google Home and Amazon Echo, has triggered an increasing interest in platforms with co-located microphone arrays and cameras. Only a few works focus on audio-visual 3D person tracking with small-size sensor configurations, such as for example a microphone pair combined with a stereo pair [10, 11].

Unlike spatially distributed sensors, a compact configuration with a small number of co-located sensors facilitates audio-visual synchronization and calibration and can be used on a moving platform, such as a robot. However, using compact co-located sensors leads to several challenges in person tracking. In addition to reverberation, background noise and abrupt person motion, other challenges include occlusions and the limited FoV of the camera. Moreover, unlike methods that use a depth sensor [12–14], when using a monocular camera and a circular microphone array (see Fig. 1(a)) we cannot derive accurate 3D location estimates, especially in complex scenarios such as when a distant target moves quickly and is not facing the platform. We therefore aim to exploit multi-modal information to improve tracking performance and to overcome the limitations of co-located sensor setups.

In this paper, we propose a novel 3D person tracker that uses audio-visual signals captured by a sensor platform consisting of an 8-element circular microphone array co-located with a monocular camera. We extract three sources of information from the audio-visual streams. First, we estimate the 3D position of the mouth geometrically with a face detector and the camera projection model. When face detections are unavailable, we resort to a color-based measurement using a reference image that, however, cannot provide information on the distance of the person from the platform. We then use audio as complementary cue to strengthen the 3D position estimation, in particular when the face detector fails or the person is outside the FoV of the camera, and to eliminate distractors such as other people or false-positive detections. We use the previously estimated height of the mouth from the video to constrain the audio search space on a 2D plane and to reduce the audio uncertainties to estimate the distance of the person from the platform. After the modality-dependent processing stages, information is fused in a particle filter that estimates the 3D position of the target mouth.

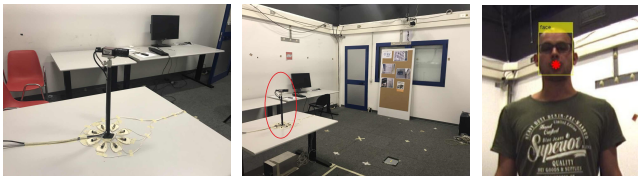

(a) (b) (c)

Fig. 1. (a) The co-located sensor platform consisting of an 8-element circular microphone array and a camera; (b) the experimental environment (the red ellipse indicates the sensor platform); and (c) an example of mouth position estimate (red dot).

2. PROPOSED AUDIO-VISUAL TRACKER

We aim to track the 3D position, $\mathbf{p}_t$, of the mouth of a person over time t, given audio signals, $\mathbf{s}_t$, captured by an 8-microphone circular array and frames, I_t, captured by a monocular camera.

We first evaluate a probability $P(\mathbf{p} \mid \mathbf{s}_{1:t}, I_{1:t})$ conditioned on past and current observations and then infer the target state from P via expectation:

$$\hat{\mathbf{p}}_t = \mathbb{E}_P(\mathbf{p} \mid \mathbf{s}_{1:t}, I_{1:t})\,. \tag{1}$$

When the signal formation $\mathbf{p} \mapsto \mathbf{s}, I$ is non-linear, incomplete and non-invertible as in our case, a common choice is a Bayesian model. Using Bayes' rule, the total probability theorem and the Chapman-Kolmogorov recursion, the model for P is fully specified by a data likelihood L, a first–order dynamics Q and an initial density P_0 [15]:

$$P(\mathbf{p} \mid \mathbf{s}_{1:t}, I_{1:t}) \propto L(\mathbf{s}_t, I_t \mid \mathbf{p}) \int Q(\mathbf{p} \mid \mathbf{q})\; P(\mathbf{q} \mid \mathbf{s}_{1:t-1}, I_{1:t-1})\, d\mathbf{q}. \tag{2}$$

The only requirement is on L and Q to be evaluable point-wise, yielding a model that is flexible and computationally attractive if

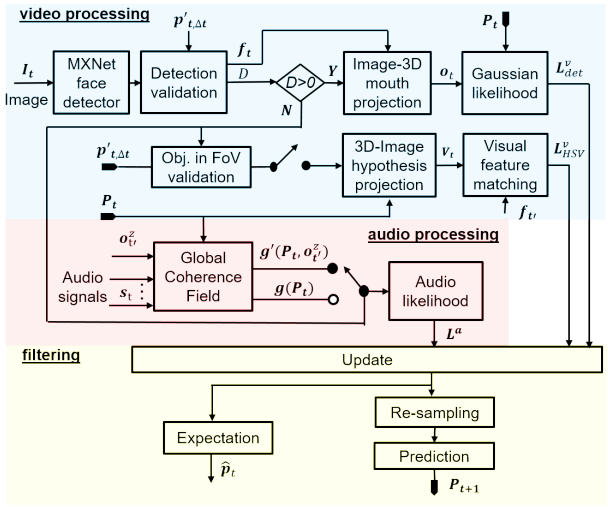

Fig. 2. Block diagram of the proposed audio-visual 3D tracker.

combined with sampling methods. We realize Eq. 2 with a Particle Filter (PF) [15], which maintains a non-parametric representation of P by propagating a set of N independently and identically distributed (iid) samples (*particles*) from P, i.e.,

$$\{\mathbf{p}_t^{(1)}, ..., \mathbf{p}_t^{(N)}\} \overset{\text{iid}}{\sim} P(\mathbf{p} \mid \mathbf{s}_{1:t}, I_{1:t}) \,. \tag{3}$$

This is achieved in two steps by (i) sampling from the prior mixture $\sum_n^N Q(\mathbf{p} \mid \mathbf{p}_{t-1}^{(n)})$ and (ii) re-sampling with probability $\propto L(\mathbf{s}_t, I_t \mid \mathbf{p})$.

We assume, as common in multi-modal tracking, conditional independence between modalities given the target state. The re-sampling probability is thus the product of the audio likelihood $L^a(\mathbf{s}_t \mid \mathbf{p})$ and the video likelihood $L^v(I_t \mid \mathbf{p})$.

Our solution comprises the modelling of the individual likelihoods, L^v, L^a (Sec. 2.1 and 2.2), and the propagation scheme and model Q (Sec. 2.3). Figure 2 shows the block diagram of the proposed tracker.

2.1. Visual observation

The proposed mouth tracker uses a face detector to derive the 3D mouth position with simple geometric considerations using prior knowledge of the typical size of a human face[1].

Let $\mathbf{f}_t^d = [u, v, w, h]^T$ be the bounding box of the d^{th} detected face, with $d = 1, \ldots, D$, at time t, where (u, v) is the position of the top left corner and (w, h) are width and height. We geometrically extract the mouth position, $\boldsymbol{\rho}_t^d = [u + 0.5w, v + 0.75h]^T$, and then use the pinhole camera model and calibration information to obtain its 3D location. We determine the scaling factor by modelling the shape of a face with a rectangle oriented towards the camera and the prior knowledge on the face width W to obtain via image-to-3D back-projection[2] the 3D mouth position: $\mathbf{o}_t^d = \Psi\left[\boldsymbol{\rho}_t^d; w, W\right]$.

Next, we validate the output of the face detector with:

$$||\boldsymbol{\rho}_t^d - \mathbf{p}'_{t,\Delta t}||_2 \leq \lambda\sqrt{w^2 + h^2}, \tag{4}$$

where λ controls the acceptable error range and $\mathbf{p}'_{t,\Delta t}$ is the average estimated mouth position on image plane in the last Δt frames.

We use spherical coordinates to better model the higher inaccuracy in the distance estimation, which is based on the hypothesised face width W. Let $\tilde{\mathbf{o}}_t^d$ and $\tilde{\mathbf{p}}$ be the estimated mouth position and a generic 3D point in spherical coordinates. Assuming a Gaussian distribution of the estimates, we evaluate the likelihood of the hypothesis p as:

$$L_{\text{det}}^v(I_t \mid \mathbf{p}) = \sum_{d=1}^{D} \exp\left[-\left(\tilde{\mathbf{o}}_t^d - \tilde{\mathbf{p}}\right)\Sigma_v^{-1}\left(\tilde{\mathbf{o}}_t^d - \tilde{\mathbf{p}}\right)^T\right], \tag{5}$$

where Σ_v accounts for the different estimation accuracy in the three spherical coordinates.

When the face is not visible or the face detector fails, we resort to a generative model and evaluate a color-based likelihood. First, we map each 3D hypothesis (particle) to the image plane by creating a bounding box using a 3D hyperrectangle oriented towards the camera $\mathbf{v} = \Phi\left[\mathbf{b}\left(\mathbf{p}; W, H\right)\right]$, where $\mathbf{b}(\mathbf{p}; W, H)$ is the 3D rectangle created from a generic 3D point $\mathbf{p}$ with face width W and height H and Φ indicates the 3D-to-image projection.

Then, we compare the color features of the bounding box with a reference image (which is updated to the last detection $\mathbf{f}_{t'}$) of the person using a Hue-Saturation-Value (HSV) spatiogram [16]. We measure the similarity $L_{\text{HSV}}^v(I_t \mid \mathbf{p})$ between two spatiograms using [17], which is derived from the Bhattacharyya coefficient.

Finally, we define the *visual likelihood* as:

$$L^v(I_t \mid \mathbf{p}) = \begin{cases} L_{\text{det}}^v(I_t \mid \mathbf{p}) & \text{if } D > 0 \\ L_{\text{HSV}}^v(I_t \mid \mathbf{p}) & \text{if } \mathbf{p}'_{t,\Delta t} \in I^{0.9} \\ 1/N & \text{otherwise,} \end{cases} \tag{6}$$

where $I^{0.9}$ is a rectangular crop corresponding to the central 90% region of the image. If $\mathbf{p}'_{t,\Delta t}$ is within this region, the person is assumed inside the camera FoV.

2.2. Video driven acoustic observations

Acoustic source localization can be accomplished by combining the information of M microphone pairs to obtain acoustic maps that represent the plausibility of an active sound source to be at a given spatial position [18].

Let the source be in $\mathbf{p}$ and $\tau_m(\mathbf{p})$ be the expected Time Difference of Arrival (TDoA) between the microphones of the m^{th} pair. If $C_m(\cdot)$ is the Generalized Cross Correlation PHAse Transform (GCC-PHAT) function computed at the m^{th} microphone pair [19, 20], then the Global Coherence Field (GCF) can be evaluated at each position $\mathbf{p}$ as [21]:

$$g(\mathbf{p}) = \frac{1}{M}\sum_{m=0}^{M-1} C_m\left(\tau_m(\mathbf{p})\right). \tag{7}$$

While a position estimate of the sound source can be obtained from the maximum of the GCF acoustic map, when a compact microphone array is employed, GCF cannot provide accurate 3D estimations, in particular along the range dimension. This problem can be overcome when some knowledge about the mouth height is available. Therefore, we design a video-driven GCF, $g'(\mathbf{p}, o_{t'}^z)$, computed by projecting a generic 3D point $\mathbf{p}$ onto the 2D plane through the mouth height $o_{t'}^z$, estimated at frame t' with the most recent face detection.

[1] Size variations of the human face are much smaller than those of other body parts (e.g. upper-body), thus allowing a more accurate 3D inference.

[2] The back-projection error is stable when $W \in [0.13, 0.15]$ m.

Finally, we define the *audio likelihood* as:

$$L^a(\mathbf{s}_t \mid \mathbf{p}) = \begin{cases} g(\mathbf{p}) & \text{if } D > 0,\ \max_{\mathbf{p}} g(\cdot) \geq \vartheta_a \\ g'(\mathbf{p}, o^z_{t'}) & \text{if } D = 0,\ \max_{\mathbf{p}} g'(\cdot) \geq \vartheta_a \\ 1/N & \text{otherwise,} \end{cases} \quad (8)$$

where $g(\cdot)$ is the previous g related variable in the brace and ϑ_a is a threshold used to remove unreliable audio observations due to pauses, noise or narrow-band spectral content.

In case of multiple detections, we select $o^z_{t'}$ as the closest one to the 3D point $\mathbf{p}$ under analysis.

2.3. Prediction

Given the audio and visual likelihoods defined above, and assuming conditional independence across the modalities, we approximate the posterior in Eq. 2 from the particle set at time $t-1$ by sampling the random variable $\mathbf{p}$ from

$$\{\mathbf{p}_t^{(1)}, ..., \mathbf{p}_t^{(N)}\} \overset{\text{iid}}{\sim} L^a(\mathbf{s}_t \mid \mathbf{p}) L^v(I_t \mid \mathbf{p}) \sum_{n=1}^{N} \mathcal{N}\left(\mathbf{p}; \mathbf{p}_{t-1}^{(n)}, 3^{\kappa}\Sigma_r\right). \quad (9)$$

Here, we model first-order dynamics Q (Eq. 2) as a mixture of Gaussian distributions whose covariance matrix Σ_r is diagonal. The value of $\kappa = 1$ if the likelihood product is in the lower 10% (higher prediction speed for low-scoring hypotheses), otherwise $\kappa = 1$.

Finally, the 3D position estimate of the mouth is the empirical expectation that approximates Eq. 1:

$$\hat{\mathbf{p}}_t = \frac{1}{N} \sum_{n=1}^{N} \mathbf{p}_t^{(n)}. \quad (10)$$

In the next section we validate the proposed tracker and compare it with alternative solutions.

3. EXPERIMENTS

We compare the proposed tracker against the audio-visual trackers in [22] and in [3], as well as with trackers that use individual modalities only, namely Audio-Only (AO) and Video-Only (VO). To account for the probabilistic nature of the PF framework, we consider the average Mean Absolute Error (MAE) (in m) for 10 runs and the Tracking Success Rate (TR), which is the percentage of frames where the error is smaller than 0.4 m.

Datasets. We use the publicly available AV16.3 dataset [23] to allow a comparison with the literature and we also collected a new dataset, FBKAV, with co-located sensors. Fig. 3 shows sample frames of the two datasets. In AV16.3, the video is captured by 3 cameras at 25 Hz with resolution of 360×288 pixels and audio is recorded at 16 kHz using two 8-element circular microphone arrays with 10 cm radius. In our experiments we use only one camera and one microphone array from the sequences $seq08$, $seq11$ and $seq12$. In FBKAV, the co-located sensors consist of an Allied Marlin F-080C camera and an 8-element circular array with omnidirectional microphones with 10 cm radius. The array is placed on a table in a room of size $4.77 \times 5.95 \times 4.5$ m (Fig. 1(b)). The room reverberation time is 0.7 s [18] and audio signals are recorded at 96 kHz. Video is captured at 15 Hz with resolution 1024×768 pixels. Synchronization and calibration are generated manually. The 3D annotation data is generated from a spatially distributed sensor set-up consisting of four Allied cameras at the corners of the room using *SmarTrack* [24]. The accuracy error of this annotation is smaller than 10 cm. We use four sequences of around one minute each: (1) 'easy': a person moves mostly in the FoV and talks facing the sensor platform; (2) '2-people': the first person always talks and moves while another silent person enters the FoV; (3) 'behind': a person exits the FoV, walks behind the camera while talking and then re-enters the FoV; (4) 'poses': a person always talks from within the FoV in a variety of challenging poses (e.g. not facing the camera, bending).

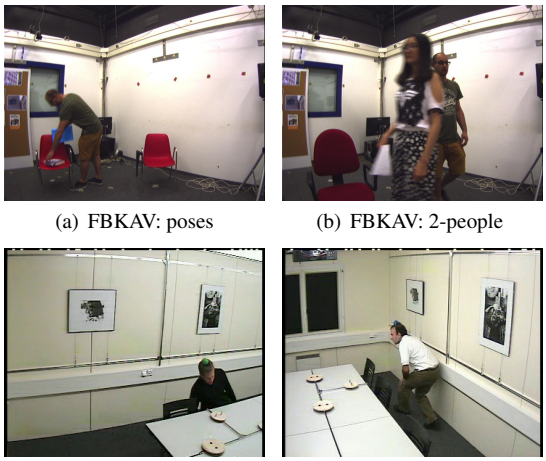

(a) FBKAV: poses (b) FBKAV: 2-people

(c) AV16.3: seq11-cam1 (d) AV16.3: seq12-cam3

Fig. 3. Sample frames from the FBKAV (a-b) and the AV16.3 (c-d) datasets.

Implementation details. We detect faces with an MXNet implementation of light CNN[3] [25]. The face width is $W = 0.14$ m and height is $H = 0.18$ m. The spatiogram in the HSV color space has 8 bins per channel; $\lambda = 2.5$, $\Delta t = 3$ and Σ_v in Eq. 5 is a diagonal matrix with elements (2°,2°,0.4 m). We compute GCC-PHAT using a 2^{10}-point and a 2^{15}-point Hanning window in AV16.3 and in FBKAV, respectively. The overlapping factor between two consecutive windows is set to provide one-to-one audio-visual frame correspondence. The validation threshold ϑ_a in Eq. 8 is set to 0.1 in AV16.3, and 0.03 in FBKAV. Different parameter settings result from their different sampling frequency. All the microphone pairs (M=28) within the 8-element array are used to obtain the GCF acoustic map. Finally, the diagonal elements of the prediction matrix Σ_r are set to $(1, 1, 0.5)$ m/s. We use 100 particles to perform 3D tracking.

Discussion. Table 1 compares the results of the proposed Audio-Visual (AV) 3D tracker with AO, VO, and [22]. For AO, we consider only 2D tracking fixing the mouth height at 1.5 m. In 'easy', AO and VO perform similarly to AV (with AO using knowledge of the height of the mouth). In '2-people', VO and AV perform well because of the face validation stage that removes false positives from the silent person. In 'behind', neither AO nor VO performs satisfactorily, because the person is outside the FOV for half of the sequence and is silent for long intervals when inside the FoV. In this case the proposed audio-visual tracker outperforms the two individual modalities. For [22], during miss-detections, tracking only relies on the 3D audio location estimates, which are inaccurate without the speaker height information. Fig. 4 shows the AV tracking results for 'behind' and its superiority over AO and VO. The sequence 'poses' includes very challenging audio situations with the person arranging

[3] https://github.com/tornadomeet/mxnet-face

Table 1. Tracking results (MAE: Mean Absolute Error in m) on the FBKAV dataset.

	AO (2D)	VO	[22]	AV
easy	.13±.01	.15±.01	.31±.01	.15±.01
2-people	.32±.04	.18±.01	.50±.01	.18±.01
behind	.43±.04	1.07±.43	.52±.01	.26±.02
poses	.95±.03	.33±.02	.80±.01	.42±.02
average	.46±.03	.43±.12	.53±.01	.25±.01

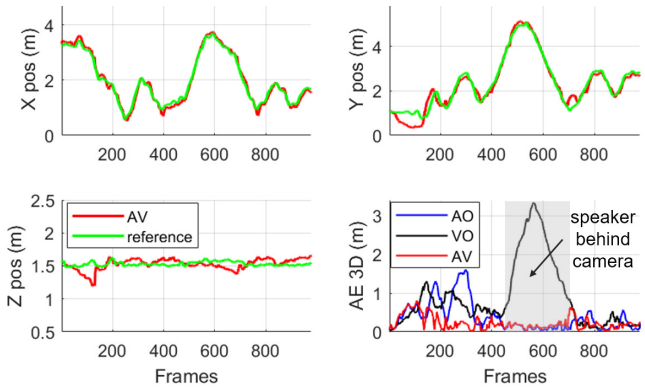

Fig. 4. AV tracking results in X,Y and Z coordinates and (bottom right) 3D Absolute Error (AE) for AO, VO and AV in 'behind'.

Table 2. Face detection success rate, DR, and tracking success rate, TR, on FBKAV.

	DR (%)	TR (%)			
		AO (2D)	VO	[22]	AV
easy	70.94	98.03	98.88	74.08	97.17
2-people	80.25	75.18	94.80	44.56	93.81
behind	48.41	62.69	48.24	40.88	81.05
poses	48.02	14.41	71.81	15.08	64.64
average	61.91	62.58	78.43	43.65	84.17

objects and facing away from the microphone array. As a result, the performance of AO considerably deteriorates with respect to the other sequences, in particular along the range dimension, and affects the AV tracking, which performs slightly worse than VO. Overall, an average 3D error of 0.25 m was obtained on the four sequences, which outperforms [22].

Table 2 reports the TR and the face detection rate, DR (i.e. the ratio between number of true positives frames and the total number of frames). Note that although the proposed method heavily relies on the face detector for the visual likelihood, the VO and AV results are always superior.

Fig. 5 quantifies the sensitivity of the proposed AV tracker to the face detection results. In 'easy', both modalities perform well and the accuracy is unaffected by the removal of the face detection results. For the other sequences, the MAE in 3D increases when the number of removed detections increases, thus leading to a performance close to the AO (2D) case. This deterioration becomes evident only when at least 50% of the detections are removed.

Table 3 shows the results in 3D and on the image plane on $seq08$, $seq11$ and $seq12$ of AV16.3, over three different camera views, and compares them with the audio-visual tracker in [3] and in [22]. For

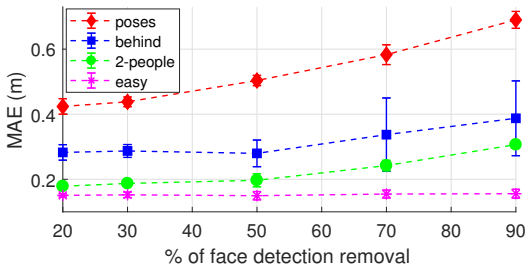

Fig. 5. Sensitivity of the proposed method (3D tracking accuracy) to the reduction of detected faces.

Table 3. Audio-visual tracking results in 3D and on the image plane on AV16.3, camera 1, 2, 3. Standard deviation is reported for the image plane only. In 3D the standard deviation is always < 0.04.

		MAE (m)		MAE (pixels)	
seq	cam	[22]	AV	[3]	AV
08	1	.15	.12	10.75 ± 0.13	4.31 ± 0.20
	2	.24	.11	7.33 ± 0.09	4.66 ± 0.09
	3	.20	.09	9.85 ± 0.12	5.34 ± 0.13
11	1	.31	.33	14.66 ± 0.34	8.15 ± 0.71
	2	.29	.14	14.01 ± 0.12	7.48 ± 0.53
	3	.26	.12	13.96 ± 0.23	6.64 ± 0.15
12	1	.41	.26	12.49 ± 0.16	6.86 ± 0.42
	2	.51	.17	10.81 ± 0.24	10.67 ± 2.00
	3	.47	.20	11.86 ± 0.24	9.71 ± 3.20
average		.32	.17	11.75 ± 0.19	7.09 ± 0.83

the latter, we fit the audio-visual likelihoods into our particle filtering framework with the same parameters used for tracking. Additionally, we replace the Viola-Jones upper-body detector [26] with the MXNet face detector. The overall 3D tracking accuracy is improved from 0.32 m to 0.17 m. When tracking on the image plane, the proposed method also outperforms [3] in every sequence with the MAE improved from 11.75 to 7.09 pixels.

4. CONCLUSION

We propose a novel 3D audio-visual person tracker that uses small-size co-located audio-visual set up. The tracker exploits the complementarity of audio and visual signals, and combines a face detector, 3D hypothesis mapping, and video-assisted audio likelihood computation. In particular, when no detection is available, we use the most recent face detection to indicate the most likely mouth height where to compute a 2D acoustic map. In addition to the tracker, we also collected a new audio-visual dataset and its annotation that we will make available to the research community.

Acknowledgment. We thank L. Cristoforetti and D. Giordani for their help in the data collection.

References

[1] Matthew J. Beal, Nebojsa Jojic, and Hagai Attias, "A graphical model for audiovisual object tracking," *IEEE Trans. on Pattern Analysis and Machine Intell.*, vol. 25, no. 7, pp. 828–836, 2003.

[2] Huiyu Zhou, Murtaza Taj, and Andrea Cavallaro, "Target detection and tracking with heterogeneous sensors," *IEEE Journal of Selected Topics in Signal Processing*, vol. 2, no. 4, pp. 503–513, 2008.

[3] Volkan Kılıç, Mark Barnard, Wenwu Wang, and Josef Kittler, "Audio assisted robust visual tracking with adaptive particle filtering," *IEEE Trans. on Multimedia*, vol. 17, no. 2, pp. 186–200, 2015.

[4] Israel D. Gebru, Silèye Ba, Georgios Evangelidis, and Radu Horaud, "Audio-visual speech-turn detection and tracking," in *International Conference on Latent Variable Analysis and Signal Separation*, August 2015, pp. 143–151.

[5] Eleonora D'Arca, Neil M. Robertson, and James Hopgood, "Person tracking via audio and video fusion," in *Data Fusion & Target Tracking Conf.: Alg. & App.*, May 2012, pp. 1–6.

[6] Dmitry N. Zotkin, Ramani Duraiswami, and Larry S. Davis, "Joint audio-visual tracking using particle filters," *EURASIP J. on Applied Signal Processing*, vol. 2002, no. 1, pp. 1154–1164, 2002.

[7] Kai Nickel, Tobias Gehrig, Rainer Stiefelhagen, and John McDonough, "A joint particle filter for audio-visual speaker tracking," in *Proc. of Int. Conf. on Multimodal Interfaces*, October 2005, pp. 61–68.

[8] Roberto Brunelli, Alessio Brutti, Paul Chippendale, Oswald Lanz, Maurizio Omologo, Piergiorgio Svaizer, and Francesco Tobia, "A generative approach to audio-visual person tracking," in *Int. Evaluation Workshop on Classification of Events, Activities and Relationships*. Springer, 2006, pp. 55–68.

[9] Alessio Brutti and Oswald Lanz, "A joint particle filter to track the position and head orientation of people using audio visual cues," in *Proc. of European Signal Processing Conference*, August 2010, pp. 974–978.

[10] Ulrich Kirchmaier, Simon Hawe, and Klaus Diepold, "Dynamical information fusion of heterogeneous sensors for 3D tracking using particle swarm optimization," *Information Fusion*, vol. 12, no. 4, pp. 275–283, 2011.

[11] Fakheredine Keyrouz, Ulrich Kirchmaier, and Klaus Diepold, "Three dimensional object tracking based on audiovisual fusion using particle swarm optimization," in *Int. Conference on Information Fusion*, Cologne, Germany, June 2008, pp. 1–5.

[12] Nagasrikanth Kallakuri, Jani Even, Yaileth Morales, Carlos Ishi, and Norihiro Hagita, "Probabilistic approach for building auditory maps with a mobile microphone array," in *Proc. of IEEE Int. Conf. on Robotics and Automation*, May 2013, pp. 2270–2275.

[13] Nagasrikanth Kallakuri, Jani Even, Yaileth Morales, Carlos Ishi, and Norihiro Hagita, "Using sound reflections to detect moving entities out of the field of view," in *Proc. of IEEE/RSJ Int. Conf. on Intelligent Robots and Systems*, November 2013, pp. 5201–5206.

[14] Jani Even, Yaileth Morales, Nagasrikanth Kallakuri, Jonas Furrer, Carlos Toshinori Ishi, and Norihiro Hagita, "Mapping sound emitting structures in 3d," in *Proc. of IEEE Int. Conf. on Robotics and Automation*, June 2014, pp. 677–682.

[15] Sanjeev M. Arulampalam, Simon Maskell, Neil Gordon, and Tim Clapp, "A tutorial on particle filters for online nonlinear/non-gaussian bayesian tracking," *IEEE Trans. on Signal Processing*, vol. 50, no. 2, pp. 174–188, Feb 2002.

[16] Stanley T. Birchfield and Sriram Rangarajan, "Spatiograms versus histograms for region-based tracking," in *Proc. of Int. Conf. on Computer Vision and Pattern Recognition*, June 2005, pp. 1158–1163.

[17] Ciaran O. Conaire, Noel E. O'Connor, and Alan F. Smeaton, "An improved spatiogram similarity measure for robust object localisation," in *Proc. of IEEE Int. Conf. on Audio, Speech and Signal Processing*, April 2007, pp. 1069–1072.

[18] Alessio Brutti, Maurizio Omologo, and Piergiorgio Svaizer, "Multiple source localization based on acoustic map deemphasis," *EURASIP Journal on Audio, Speech, and Music Processing*, vol. 2010, no. 11, January 2010.

[19] Maurizio Omologo and Piergiorgio Svaizer, "Acoustic event localization using a crosspower-spectrum phase based technique," in *Proc. of IEEE Int. Conf. on Audio, Speech and Signal Processing*, April 1994, pp. 273–276.

[20] Charles Knapp and Glifford Carter, "The generalized correlation method for estimation of time delay," vol. 24, no. 4, pp. 320–327, 1976.

[21] Maurizio Omologo, Piergiogio Svaizer, and Renato De Mori, "Acoustic transduction," in *Spoken Dialogue with Computer*, Renato De Mori, Ed., chapter 2, pp. 1–46. Academic Press, 1998.

[22] Xinyuan Qian, Alessio Brutti, Maurizio Omologo, and Andrea Cavallaro, "3D audio-visual speaker tracking with an adaptive particle filter," in *Proc. of IEEE Int. Conf. on Audio, Speech and Signal Processing*, March 2017, pp. 2896–2900.

[23] Guillaume Lathoud, Jean-Marc Odobez, and Daniel Gatica-Perez, "AV16.3: an audio-visual corpus for speaker localization and tracking," in *Machine Learning for Multimodal Interaction*, pp. 182–195. Springer, June 2004.

[24] Oswald Lanz, "Approximate bayesian multibody tracking," *IEEE Trans. on Pattern Analysis and Machine Intell.*, vol. 28, no. 9, pp. 1436–1449, July 2006.

[25] Xiang Wu, Ran He, and Zhenan Sun, "A lightened CNN for deep face representation," *arXiv preprint arXiv:1511.02683*, 2015.

[26] Paul Viola and Michael Jones, "Robust real-time face detection," *International Journal of Computer Vision*, vol. 57, pp. 137–154, 2004.